HAL
open science

# Oxygen and water vapor permeability of fully substituted long chain cellulose esters (LCCE)

Julien Bras, Carlos Vaca-Garcia, Marie-Elizabeth Borredon, Wolfgang Glasser

## To cite this version:

Julien Bras, Carlos Vaca-Garcia, Marie-Elizabeth Borredon, Wolfgang Glasser. Oxygen and water vapor permeability of fully substituted long chain cellulose esters (LCCE). Cellulose, 2007, 14 (4), pp.367-374. 10.1007/s10570-007-9123-2 . hal-02058611

**HAL Id: hal-02058611**

**https://hal.science/hal-02058611v1**

Submitted on 6 Mar 2019

**HAL** is a multi-disciplinary open access archive for the deposit and dissemination of scientific research documents, whether they are published or not. The documents may come from teaching and research institutions in France or abroad, or from public or private research centers.

L'archive ouverte pluridisciplinaire **HAL**, est destinée au dépôt et à la diffusion de documents scientifiques de niveau recherche, publiés ou non, émanant des établissements d'enseignement et de recherche français ou étrangers, des laboratoires publics ou privés.

Open Archive Toulouse Archive Ouverte (OATAO)

OATAO is an open access repository that collects the work of Toulouse researchers and makes it freely available over the web where possible

This is an author's version published in: http://oatao.univ-toulouse.fr/23056

**Official URL:** https://doi.org/10.1007/s10570-007-9123-2

**To cite this version:**

Bras, Julien and Vaca-Garcia, Carlos and Borredon, Marie-Elizabeth and Glasser, Wolfgang *Oxygen and water vapor permeability of fully substituted long chain cellulose esters (LCCE).* (2007) Cellulose, 14 (4). 367-374. ISSN 0969-0239

Any correspondence concerning this service should be sent to the repository administrator: tech-oatao@listes-diff.inp-toulouse.fr

DOI 10.1007/s10570-007-9123-2

# Oxygen and water vapor permeability of fully substituted long chain cellulose esters (LCCE)

**Julien Bras · Carlos Vaca-Garcia · Marie-Elizabeth Borredon · Wolfgang Glasser**

**Abstract** Fully-substituted cellulose esters with acyl substituents ranging in size from C2 to C18 were synthesized using the acyl chloride method. Films were prepared from the purified esters by either solvent-casting or compression-molding at elevated temperatures. Oxygen and water vapor permeability was determined under different conditions of pressure and moisture. The relationship between cellulose ester structure and barrier properties was examined. The results revealed linear relationships between water vapor and oxygen permeabilities and molar ester substituent volume as well as several structural factors relating to polymer polarity and hydrophobicity, such as aliphatic (methylene) content, solubility parameter, and contact angle. Films from long chain cellulose esters (LCCE) with acyl substituents in the size range between C8 and C18 were found to represent effective barriers to water vapor transport while their obstruction to the transfer of oxygen remained low. It was concluded that the hydrophobic nature of LCCEs is responsible for the control of water vapor transport, and that spatial factors dominate the transfer of oxygen.

**Keywords** Long chain cellulose esters · Oxygen permeability · Water vapor permeability · Barrier polymer properties

J. Bras (✉)
Laboratoire de Génie des Procédés Papetiers (UMR 5518 CNRS-CTP-INPG), Institut National Polytechnique de Grenoble, 461 Rue de la papeterie, 38402 St Martin d'Hères, France
e-mail: Julien.Bras@efpg.inpg.fr

C. Vaca-Garcia · M.-E. Borredon
Laboratoire de Chimie Agro-Industrielle, (UMR 1010 INRA/INP-ENSIACET), Institut National Polytechnique de Toulouse, 118, route de Narbonne, 31077 Toulouse Cedex 04, France

W. Glasser
Department of Wood Science and Forest Products, Virginia Tech, Blacksburg, VA, USA

## Introduction

Most synthetic polymers used in packaging are vital to such aspects as material handling, food safety and preservation, and human health while presenting serious disposal problems. Biopolymers, such as cellulose and its derivatives, may offer attractive alternatives as long as their properties can be tailored to specific end-use applications. Permeability to oxygen and moisture, and mechanical properties, rank high among the performance criteria of barrier polymers (Petersen et al. 1999). Regenerated cellulose and cellulose derivatives have been widely studied, and there are numerous industrial applications in fiber, film and gel-based materials. For example, cellulose ethers are used in the preparation of edible films with efficient oxygen and hydrocarbon

barrier properties (Kamper and Fennema 1984; Park et al. 1993). The knowledge about the behavior of cellulose esters, however, is incomplete. While cellulose esters possess very well-known thermoplastic properties (Wang and Tao 1995; Sealey et al. 1996; Vaca-Garcia et al. 2003), their characteristics as barrier polymers remain obscure. Whereas short chain cellulose esters, such as cellulose acetate, cellulose propionate and cellulose butyrate as well as cellulose acetate butyrate (mixed ester) have received much attention in the technical, trade and patent literature for several decades (Stannett 1950; Fisher 1959; Glasser et al. 1995; Edgar et al 2001; Heinze et al. 2003; Rustemeyer 2004; Heinze et al 2006), long chain cellulose esters (LCCE) have only recently captured much attention. Excellent reviews have been provided by Edgar et al. (2001) and Heinze et al. (2006).

It is known that such properties as solvent solubility, mechanical strength, melt viscosity, thermal transitions, and others, of LCCE are greatly dependent on both the degree of substitution (DS) and the type of substituent (i.e., size of the ester group, number of methylene groups, etc.).

Our objective was to explore the qualifications of LCCEs as barrier polymers. Since the chemical properties of LCCEs are subject to wide variation, permeability to oxygen and water vapor can be expected to be adjustable to specific end-use applications as well.

## Materials and methods

### Materials

α-Cellulose from Sigma (France) (DP = 960, 4% pentosans) was used for the synthesis of the LCCEs. Fatty acid chlorides, pyridine, and other chemicals were certified reagent-grade (Aldrich, France). They were used without further purification. Methyl and ethyl cellulose (DS = 3), cellulose triacetate and hydroxypropylcellulose (MS = 10, M.w. = 100,000) were purchased from Aldrich.

### LCCE synthesis

The acid chloride/pyridine method reported by Vaca-Garcia et al. (2000) was employed with minor modification. All of the samples were prepared under identical conditions of temperature and reaction time in order to obtain comparable DP values (not measured). The amount of acyl chloride was adjusted so as to reach the highest DS-values. Cellulose (10 g) was stirred in excess pyridine (250 mL) at 20 °C for 30 min. Fatty acid chloride (2 equiv/OH) was poured into the reaction vessel, and the mixture was refluxed at 130 °C for 2 h with mechanical stirring. After cooling to 100 °C, 250 mL of 50% aqueous ethanol were added in order to consume excess acid chloride and to precipitate the cellulose derivatives that had transitioned into homogeneous phase. The powderous product was recovered by filtration (sintered glass filter) and washing with ethanol and acetone. After further purification by Soxhlet extraction with acetone (or with ethanol if the derivative was acetone-soluble) for 16 h, the cellulose ester was dried at 50 °C to constant weight and stored in a desiccator at room temperature. DS was determined by elemental analysis according to an earlier report (Vaca-Garcia et al. 2001).

### Compression-molded Films

Cellulose ester films were prepared by compression-molding at temperatures of ca. 20 °C above glass-transition temperature ($T_g$) between Teflon® sheets using a heated laboratory press (4 tons). The mould was rapidly cooled by flushing the press platens with cold water so as to preserve a disordered morphology. Film size was maintained at 60 $cm^2$ and film thickness averaged 200 μm.

### Solvent-cast films

A solution of cellulose ester in chloroform ($CHCl_3$, 1% w/v), the solvent determined to be widely applicable from solubility tests, was prepared by stirring the ester at room temperature for 24 h. An appropriate amount of solution to yield a film of the desired size (60 $cm^2$) and thickness (50 μm) was poured into a glass Petri box and allowed to stand at room temperature.

### Quality control testing of films

Ensuring uniform film quality was considered to be essential. The absence of holes and other defects in the films was checked by observation with an optical

microscope; and it was further assessed by using a Parker Print Surf 90 apparatus which measures the drop of a forced air flow through the film. Ten measurements were made with each film. The absence of holes was indicated by air flow values of <10 mL/min, a value attributed to air permeability. The presence of holes was usually signified by flow values that were 1,000-times higher. Defective films were discarded.

A scanning electron microscope (LEO 435VP by Cambridge, UK) was used to assess surface homogeneity of the films. Thickness of the films was accurately measured with an automatic micrometer (Adamel Lhomargy m120) at 20 points on each film sample of 60 $cm^2$ area.

### Contact angle measurements

Surface hydrophobicity was assessed by measuring contact angle (DigiDrop, GBX, Romans-sur-Isère, France). A 5 µl drop of distilled water was placed on the surface of the film with an automatic piston syringe and photographed. An image analyzer was used to measure the angle formed between the base and the tangent of the drop. Values were obtained along with time (up to 5 min with acquisitions every 30 s), and contact angles were averaged from five measurements per film.

### Static water vapor permeability (sWVP)

Static WVP of films was determined according to ASTM standard [E96-95, 1995]. Film samples (60 $cm^2$ each) were conditioned at 25 °C and 60% RH for 24 h and then used to hermetically cover aluminum pans containing 5 mg of anhydrous calcium chloride. Toric joint seal was used to attach the film to the cup. The assembly was accurately weighed and then placed in a forced convection chamber at 25 °C and 60 % RH. The pans were weighed at regular time intervals. The relationship between the quantity of water transferred per unit area and unit of time was obtained.

After standardization for unitary film thickness, the slope of the fitted curve (straight line) allowed the calculation of the static WVP. All the tests were performed in triplicate at atmospheric pressure (1 atm) and the WVP value of each film was reported as the average of these 3 values.

$$WVP\left(\mathrm{g\ m^{-1}\ s^{-1}\ Pa^{-1}}\right) = \Delta m \times e/[A \times \Delta t \times \Delta P] \quad (1)$$

where $\Delta m$ is mass increase (in g) of the $CaCl_2$ sample; $A$ is film area ($m^2$); and $\Delta t$ represents exposure time in the chamber (s). The thickness of the film is $e$, and $\Delta P$ is the partial water vapor pressure difference across the two sides of the film specimen corresponding to 0–60% RH, i.e., 1,875 Pa.

### Dynamic water vapor permeability (dWVP)

A Mocon apparatus was used in the ''tropical condition''—mode (38 °C and 90% RH) to measure dynamic WVP. A small film sample (1 $cm^2$) separates two chambers. The principle is based on the transfer of moisture whereby first chamber is swept by a $N_2$ gas flow containing 90% RH, and the second chamber is swept by a dry $N_2$ gas flowing in the opposite direction. Three measurements were made per sample in each case.

### Oxygen permeability

ASTM standard D 3985-95 was followed to evaluate oxygen permeability.

The film sample was placed between two chambers with different oxygen partial pressures (21% and 100%). By inserting a syringe through a septum, an air sample was taken in the chamber having the lower oxygen concentration. The actual oxygen concentration was determined by gas chromatography (Shimadzu, GC-14b) with a coulometry sensor. Evolution of $P[O_2]$ with time allowed the determination of oxygen permeability. A control sample of poly(ethylene terephtalate) film was used as reference.

### Parameter calculation and definition

Different intrinsic parameters were determined by calculation. According to Vaca-Garcia et al. 2003, the cellulose were considered as a composite of cellulose polymer and fatty acid chains. The latter represent the methylene groups of the acyl substituents; that is, R′ in the following formula: $R'CH_2C(O)$-. This consideration allows the calculation of the methylene content as the mass fraction of R' in $R'CH_2C(O)$-O-cellulose.

The acyl molar volume corresponds to the volume fraction of one alkyl substituent ($V = V_{CO} + (n - 1)V_{CH2}$). This fraction functions as ''spacer'' between cellulose chains.

The solubility parameters ($\delta$) were calculated using the method of Coleman et al. (1990).

## Results and discussion

### LCCE synthesis and film preparation

The cellulose esters used in this study were synthesized to high degrees of substitution (DS) as indicated in Table 1. Several cellulose ethers were obtained from commercial sources.

Cellulose esters have high glass transition temperatures that vary with type and amount of substitution. Derivatizing cellulose with acids having alkyl chains of increasing length causes a progressive internal plasticization (Edgar et al. 1998; Vaca-Garcia et al. 2003). However, the solubility of LCCEs with high DS suffers, especially if they are prepared in heterogeneous solid-liquid medium (Edgar et al. 1998). The loss of solubility interferes with the film preparation method in which solution-casting is preferred.

Solubility tests were performed at the beginning and end of a 24 h time period during which the polymer was kept in an agitated suspension at room temperature. Some insoluble samples were gently heated to promote dissolution. Films of cellulose ester derivatives with C2 to C12 substituents were prepared by solution-casting using $CHCl_3$ as solvent. Contrary to published data (Malm et al. 1951), it was not possible to dissolve some derivatives considered to be soluble in $CHCl_3$. In these cases, films were prepared by compression-molding at elevated temperatures. Prior to hot- pressing the cellulose derivatives, their $T_g$ values were determined by DSC analysis. Films of C8, C12, C16 and C18 triesters were prepared by compression-molding at temperatures of about $T_g$ + 20C to constant thickness followed by rapid cooling in order to prevent the formation of an ordered morphology.

### Water vapor permeability (WVP) of solvent-cast films

The experimental and calculated results for all films are summarized in Table 2. Two commercial materials (cellophane and polypropylene) are included as reference materials. It is apparent that WVP varies with substituent type as well as method of film preparation. The solvent-cast film of cellulose trilaurate, for example, was significantly less permeable than the solvent cast films of cellulose derivatives bearing much shorter side-chains, such as like methyl cellulose, ethyl cellulose or cellulose triacetate (Table 2). The C12-LCCE solvent-cast film furthermore showed similar barrier properties as the hydroxypropyl cellulose film prepared by the same method. The latter is frequently used as barrier polymer in food packaging. Moreover, when comparing cellulose acetate and ethyl cellulose, which are cellulose derivatives bearing two carbon atoms in the side chains, the derivative having an ester functionality conferred better barrier properties to water vapor

**Table 1** DS and selected properties of cellulose esters and their films. DS-values were obtained by elemental analysis (duplicate determination)

| Derivatives | DS | Origin | Thermopressing temperature | Casting solvent |
|---|---|---|---|---|
| C. Acetate | 2.99 ± 0.01 | Commercial | – | $CHCl_3$ |
| C. Octanoate | 3.01 ± 0.10 | Synthesized | 90 °C | $CHCl_3$ |
| C. laurate | 3.05 ± 0.10 | Synthesized | 100 °C | $CHCl_3$ |
| C. Palmitate | 2.97 ± 0.05 | Synthesized | 100 °C | – |
| C. Stearate | 2.90 ± 0.10 | Synthesized | 90 °C | – |
| Methyl C. | 2.90 ± 0.10 | Commercial | – | $H_2O$ |
| Ethyl C. | 2.90 ± 0.10 | Commercial | – | $H_2O$ |
| Hydroxypropyl C. | 10 ± 1 (MS) | Commercial | 100 °C | $H_2O$, Ethanol, Acetone |
| Cellophane (regenerated C.) | _ | Commercial | – | – |

**Table 2** Experimental and calculated results of solvent-cast and compression-molded films

| | n[a] | Static WVP[c] ($10^{-12}$ g m$^{-1}$ s$^{-1}$ Pa$^{-1}$) | Dynamic. WVP[c] (g m$^{-1}$ d$^{-1}$) | $O_2$ Permeability[c] (cm$^3$ m$^{-1}$ d$^{-1}$ b$^{-1}$) | $\delta$[d] Solubility Parameter | Methylene content (wt %) | Acyl molar vol[e] (cm$^3$ mol$^{-1}$) | Contact angle[f](°) |
|---|---|---|---|---|---|---|---|---|
| ESTER | 2 | 77.85 | – | – | 10.4 | 0 | 81.6 | – |
| | *8$^T$* | *31.9* | *0.28* | *0.239* | *8.9* | *46.7* | *126.2* | *103* |
| | 12 | 28.8 | – | – | 8.7 | *59.8* | 192.2 | – |
| | *12$^T$* | *19.7* | *0.18* | *0.599* | | | | *112* |
| | *16$^T$* | *7.4* | *0.09* | *0.828* | *8.5* | *67.0* | *258.2* | 113 |
| | *18$^T$* | *4.5* | *0.06* | *1.301* | *8.5* | *69.6* | *291.2* | 114 |
| ETHER | 1 | 96.1 | – | – | 9.4 | – | 49.5 | – |
| | 2 | 97.0 | – | – | 9.0 | – | 99.0 | – |
| REF | HPC[b] | 26.9 | – | – | 8.8 | – | – | – |
| | *HPC$^T$* | *22.8* | – | – | | | | |
| | Cello[b] | 24.3 | 0.11 | 0.436 | 14.0 | – | – | 70 |
| | PP[b] | 0.3 | 0.01 | – | 7.4 | – | – | – |

[a] Superscript ''T'' and italics implies that thermopressed films

[b] Cello: cellophane; HPC: HydroxyPropylCellulose, PP: Polypropylene

[c] Static and dynamic water vapor permeability (WVP) and oxygen permeability were determined as described in the experimental section

[d] The Hildebrand solubility parameter, $\delta$, was determined by by using the method of Coleman, Serman; Bhagwagar and Painter, 1990

[e] Molar volume is given in molar equivalents per AGU (162 g.mol$^{-1}$)

[f] The contact angle is determined by DigiDrop, GBX

as compared to the one bearing an ether substituent (Table 2).

## WVP of compression- molded films

The permeabilities to water vapor of compression-molded films were compared to those prepared by solution-casting (i.e., cellulose laurate, hydroxypropyl cellulose). Heat-treated films quenched by rapid cooling are expected to represent polymers with less ordered phases than films prepared by solution-casting. The results (Table 2) reveal that thermal processing helps reduce permeability to water vapor. Hot-pressed cellulose laurate films had WVP-values that were 31% lower than films prepared by solution-casting. Hot-pressed films of LCCEs with increasing substituent chain length revealed an increasing resistance to water vapor transport. These molded films have WVP-values that correlate with methylene content (Fig. 1). The static barrier behavior declines from 32 to $4.5 \times 10^{-12}$ g m$^{-1}$ s$^{-1}$ Pa$^{-1}$ when the acyl chain length increases from C8 (about 47% methylene) to C18 (about 70% methylene).

These results demonstrate that long acyl chains improve the water vapor barrier properties. This is surprising from the perspective of side chains acting as protruding spacers that separate cellulosic chains

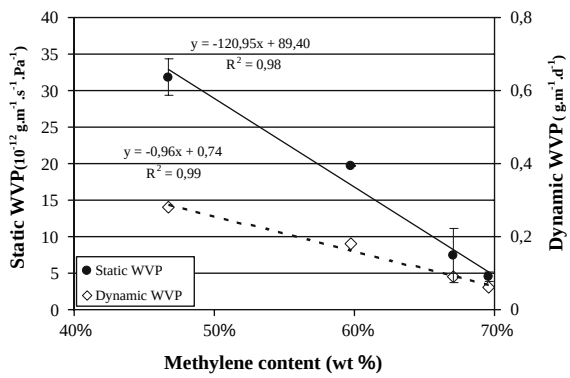


**Fig. 1** Static (25 °C, 60%RH) and Dynamic (35 °C, 90%RH) water vapor permeability of molded LCCE films vs. methylene content

as suggested by Ayranci and Tunc 2001, who suggested that long side-groups spread out cellulose chains and thereby raise the permeability to gases.

Two hypothetical explanations can be proposed to resolve this apparent contradiction. The WVP decrease may be due to the fact that the fatty chains of LCCE form an ordered phase (Sealey et al. 1996), which might impede water vapor transport. Similar observations on the relationship between water vapor permeability & the crystalline order in fat based barrier films have recently been reported by Martini et al. 2006. However, it is also possible that a hydrophobic boundary layer on the film surface creates interference.

In order to elucidate this hypothesis, we decided to circumvent the effect of a hydrophobic boundary layer by evaluating the dynamic WVP, which measures the humidity transfer rate difference of a gas flow under simulated tropical conditions. This technique uses a continuous gas flow instead of a static atmosphere. Moreover the higher relative humidity (RH) increases the potential difference between the chambers and accentuates the permeability phenomenon.

Figure 1 reveals that the water vapor barrier properties increase with the methylene content of the acid substituents under both dynamic and static conditions. This makes it evident that it is the hydrophobic character of LCCE that is most likely responsible for the character of the water vapor barrier polymer. The correlation between WVP and solubility parameter ($\delta$) (Fig. 2) provides additional support for this hypothesis. Film hydrophobicity seems to play a role by repulsing water molecules and artificially diminishing intrinsic WVP values.

Whatever the case, from a practical point of view, it is obvious that the hydrophobic character produced by the fatty acid substituents favors an increase in water vapor barrier properties of LCCE.

These results suggest that relative WVP-values can be tailored, modeled and predicted via $CH_2$-content or solubility parameter ($\delta$). This is not unexpected, but it reveals that a rigorous quantitative relationship exists for LCCEs with ester substituents in the size range of C8 to C18 and WVP. To confirm this predictive relationship, we synthesized a tridecanoate (C10) cellulose ester; we prepared a film by compression-molding; and we determined its static WVP. Determining the sWVP-behavior, we obtained

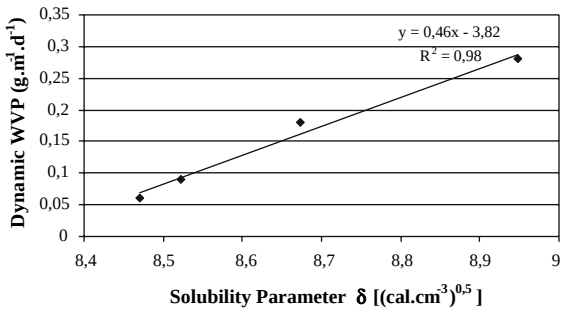


**Fig. 2** $\delta$ solubility and dynamic WVP correlation of molded LCCE

a value of $(24.885 \pm 2.054) \times 10^{-12}$ g m$^{-1}$ s$^{-1}$ Pa$^{-1}$. This compares well with the predicted values based on the relationships established for sWVP vs. molar acyl content and methylene content given in the first column of Table 3. Using the established relationships of Table 3, sWVP-values in dependence of acyl molar volume, methylene content, and solubility parameter were predicted to be ($25.766 \times 10^{-12}$ g m$^{-1}$ s$^{-1}$ Pa$^{-1}$), ($24.708 \times 10^{-12}$ g m$^{-1}$ s$^{-1}$ Pa$^{-1}$), and ($23.626 \times 10^{-12}$ g m$^{-1}$ s$^{-1}$ Pa$^{-1}$), respectively. The theoretical average then is $(24.700 \pm 1.069) \times 10^{-12}$g m$^{-1}$ s$^{-1}$ Pa$^{-1}$, which is very near the experimental value (less than 1% of difference). This result provides evidence in support of the predictive nature of at least static WVP in relation to well-defined structural features in the acyl size range of C8 to C18.

## Oxygen permeability

Since Ayranci and Tunc (2001) suggested that diffusivity of water vapor is controlled by the hydrophobicity of the barrier polymer, we considered it to be important to analyze the permeability of another gas less sensitive to surface energy differences. Therefore, we studied the permeability of oxygen, which is an important selection parameter for food packaging materials. The results (Fig. 3) provide evidence that oxygen permeability is linearly related to acyl group size (''spacer size''). Indeed, this gas passes more easily through the barrier film material when the substituent size on the LCCE polymer increases. These results are in agreement with those of Mouls (1994), who has demonstrated in work with synthetic polymers that an internal plasticizer increases oxygen permeability. Comparing oxygen permeability with WVP (Fig. 3), an opposite behavior

**Table 3** Equations and linear regression coefficient ($R^2$) of different permeabilities (Y) in relation to different structural parameters (X)

| | Y | | |
|---|---|---|---|
| | sWVP ($10^{-12}$ g $m^{-1}$ $s^{-1}$ $Pa^{-1}$) | dWVP (g $m^{-1}$ $d^{-1}$) | Oxygen permeability ($cm^3$ $m^{-1}$ $d^{-1}$ $bar^{-1}$) |
| X | | | |
| Acyl molar vol ($cm^3.mol^{-1}$) | 0.991 (y = −0.17x + 52.83) | 0.994 (y = −0.0014x + 0.47) | 0.930 (y = 0.0058x − 0.5157) |
| Flexible methylene content (%) | 0.981 (y = −120.90x + 89.40) | 0.985 (y = −0.96x + 0.74) | 0.867 (y = 4.01x − 1.69) |
| $\delta$ solubility | 0.979 (y = 57.876x − 484.96) | 0.984 (y = 0.46x − *3.82)* | 0.864 (y = −1.92x + 17.34) |
| contact angle | 0.845 (y = −2.27x + 266.94) | 0.857 (y = −0.018x + 2.15) | 0.736 (y = 0.075x − 7.52) |

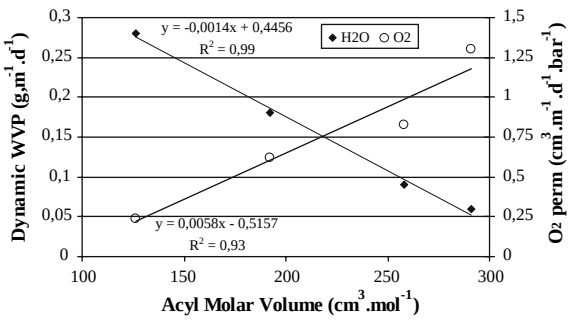


**Fig. 3** WVP (♦) and Oxygen (○) permeability of LCCE molded films

is detected between the two barrier parameters. Whereas oxygen permeability increases with substituent size, WVP decreases, probably as a result of the increase in hydrophobicity of the LCCE. It is apparent that where spatial effects dominate oxygen permeability, polarity (and solubility parameter) effects control WVP.

It can therefore be concluded that the fatty acid side-chains act as a hydrophobic barrier layer while also functioning as an internal plasticizer. The creation of space and free volume between cellulosic main chains creates permeability to oxygen while it interferes with moisture transport.

The significance of the factors relating to space, hydrophobicity and solubility parameter on barrier properties was evaluated statistically, and different correlations were derived with 4 experimental points, each. The linear regression coefficients were calculated and are presented in Table 3. The data reveal highly significant relationships that permit the conclusion that the oxygen permeability of barrier polymers based on compression-molded LCCE-films is most significantly influenced by the molar volume of the acyl substituent, whereas WVP depends mainly on the hydrophobicity (methylene content and solubility parameter). Contact angle measurements produced relationships of lower significance, probably because surface irregularties in the films.

### WVP and oxygen permeability correlation

Mouls (1994) demonstrated that the oxygen permeability of classical synthetic barrier polymers (including PP, OPP, PEHD, PEBD, PCTFE) clearly increases when WVP increases (Fig. 4B). LCCE films clearly exhibit the opposite behavior: oxygen permeability decreases as WVP increases. This is a particular behavior of LCCEs that may dramatically influence the use potential of fatty cellulose esters in packaging applications, for such products as food wrappings, which need to be protected from humidity while permitting unobstructed gas exchange.

## Conclusion

LCCEs have gas and water vapor barrier properties that are different from those of most synthestic polymers. The barrier properties to water vapor are increasingly obstructive as hydrophobicity rises whereas oxygen permeability increases.

Whereas WVP of LCCE-based films is most significantly influenced by structural factors relating to polarity and hydrophobicity (aliphatic alkyl content and solubility parameter), oxygen permeability was found to be most dramatically influenced by factors relating to space.

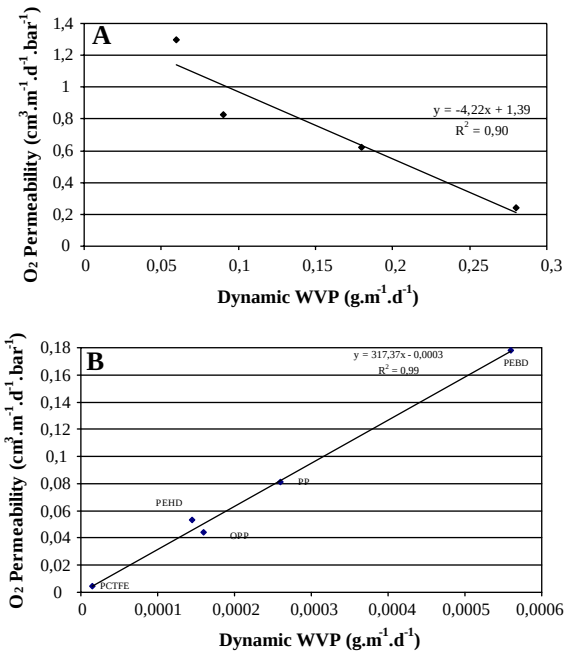


**Fig. 4** Comparison of Oxygen permeability with dynamic WVP for LCCE compression-molded films (**A**) and for synthetic barrier films (**B**) [Mouls, 1994 ]

Data from static and dynamic water vapor transport experiments using compression-molded barrier films of LCCEs having substituents in the C8 to C18 range suggest that the barrier properties of cellulose esters can be tailored on the basis of structural details.

It is expected that LCCEs have potential for the development of barrier polymers in food packaging and food preservation.

## References


ASTM Standard (1995) Standard test methods for water vapor transmission of materials. Reference ASTM E 96–95. In: Annual book of ASTM standards, American Society for Testing and Materials, vol. 4, West Conshohocken, PA, pp 697–704

Ayranci E, Tunc S (2001) The effect of fatty acid content on water vapour and carbon dioxide transmissions of cellulose-based edible films. Food Chem 72:231–236

Coleman MM, Sermann CJ, Bhagwagar DE, Painter PC (1990) Polymer reviews: a practical guide to polymer miscibility. Polymer 31:1187–1203

Edgar KJ, Pecorini TJ, Glasser WG (1998) In: Heinze TJ, Glasser WG (eds) Cellulose derivatives, pp 38–61

Edgar KJ, Buchanan CM, Debenham JS, Rundquist PA, Seiler BD, Shelton MC, Tindall D (2001) Advances in cellulose ester performance and application. Prog Polym Sci 26:1605–1688

Fisher JW (1959) Recent advances in the chemistry of cellulose and starch. In: Honeyman J (ed) Heywood, London, p 188

Glasser WG, Samaranayake G, Dumay M, Davé V (1995) Novel cellulose derivatives. III. Thermal analysis of mixed esters with butyric and hexanoic acid. J Polym Sci Part B Polym Phys 33:2045–2054

Heinze T, Liebert TF, Pfeiffer KS, Hussain MA (2003) Unconventional Cellulose Esters: Synthesis, Characterization and Structure-Property Relations. Cellulose 10:283–296

Heinze T, Liebert T, Koschella A (2006) Esterification of Polysaccharides. Springer, 232 pp

Kamper SL, Fennema O (1984) Water vapor permeability of an edible, fatty acid, bilayer film. J Food Sci 49:1482–1485

Malm CJ, Mench JW, Kendall DL, Hiatt GD (1951) Aliphatic acid esters of cellulose. Preparation by acid chloride-pyridine procedure. J Ind Eng Chem 43:684–688

Martini S, Kim DA, Ollivon M, Marangoni AG (2006) Structural factors responsible for the permeability of water vapor through fat barrier films. Food Res Int 39:550–558

Mouls JP (1994) Nature des polymères et adéquation de la barrière à l'eau et à l'oxygène. In abstract of the: ISECA Colloque 1994, pp 42–50

Park HJ, Weller CL, Vergano PJ, Testin RF (1993) Permeability and mechanical properties of cellulose-based edible films. J Food Sci 58:1361–1370

Petersen K, Nielsen PV, Bertelsen G, Lawther M, Olsen MB, Nilsson NH, Mortensen G (1999) Potential of biobased materials for food packaging. Trends Food Sci Technol 10:52–68

Rustemeyer P (2004) Cellulose Acetates: properties and application. Wiley, Germany, p 394

Sealey JE, Samaranayake G, Todd JG, Glasser WG (1996) Novel cellulose derivatives. IV. Preparation and thermal analysis of waxy esters of cellulose. J Polym Sci Part B Polym Phys 34:1613–1620

Stannett V (1950) Cellulose Acetate Plastics. Temple Press Ltd, London, p 325

Vaca-Garcia C, Borredon ME, Gaseta A (2001) Determination of the degree of substitution (DS) of mixed cellulose esters by elemental analysis. Cellulose 8:225–231

Vaca-Garcia C, Gozzelino G, Borredon ME (2000) Structure-property relationships of n-acyl esters of cellulose. In: Abstracts of 219th ACS National Meeting, San Francisco

Vaca-Garcia C, Gozzelino G, Glasser G, Borredon ME (2003) Dynamic mechanical thermal analysis transitions of partially and fully substituted cellulose fatty esters. J Polym Sci Part B Polym Phys 41:281–288

Wang P, Tao BY (1995) Synthesis of cellulose-fatty acid esters for use as biodegradable plastics. J Environ Polym Degrad 3:115–119